Highly Active Carbon Nanotube-Supported Bimetallic Palladium-Iron Electrocatalysts for Formic Acid Electro-Oxidation

Yanxian Jin[1,2,3], Chun'an Ma[2,*], Meiqin Shi[2], Youqun Chu[2], Yinghua Xu[2], Tao Huang[1], Qian Huang[1],Yiwai Miao[1]

[1] School of Pharmaceutical and Chemical Engineering, Taizhou University, Linhai 317000 ,China
[2] State Key Laboratory Breeding Base of Green Chemistry－Synthesis Technology, College of Chemical Engineering and Materials science, Zhejiang University of Technology, Hangzhou 310032, China
[3] Zhejiang Key Laboratory for Reactive Chemistry on Solid Surfaces, Institute of Physical Chemistry Zhejiang Normal University, Jinhua 321004, China
[*]E-mail: science@zjut.edu.cn; snowflakej@gmail.com

In this work, a novel nanodispersed multi-walled carbon nanotubes (MWCNTs) supported PdFe catalysts were prepared for the oxidation of formic acid in direct formic acid fuel cells (DFAFCs). According to the X-ray diffraction (XRD) and transmission electron microscopy (TEM) images, the Pd/MWCNTs catalyst has been demonstrated to significant aggregation of Pd particles with a wide particle size distribution of 2-16 nm and centers at 6.5 nm, while the 2Pd1Fe/MWCNTs (the atomic ratio of Pd and Fe = 2:1) catalyst has a relatively uniform and high dispersion of alloyed nano-PdFe and nano-FeO$_x$ metal particles in a range of 4-13 nm and centers at 8.2 nm. Intriguingly, PdFe/MWCNTs catalysts exhibit superior activity in formic acid electro-oxidation to Pd/MWCNTs catalyst. The potential of the anodic peak of formic acid at the 2Pd1Fe/MWCNTs catalyst electrode is 125 mV more negative than that and the peak current density is 52% higher than that at the Pd/MWCNTs catalyst electrode. This suggests their use has great potential in DFAFCs as highly efficient and cost-effective catalysts. The occurrence of iron can influence on the activity of catalyst by two ways.

Keywords: Electro-oxidation; Formic acid; Fuel cell; PdFe; Carbon nanotubes

1. INTRODUCTION

Direct formic acid fuel cells (DFAFCs) system is a promising candidate for a power supply for portable applications [1]. Recently, DFAFCs have attracted considerable attention due to their multiple

advantages of high electromotive force, limited fuel crossover, and high practical power densities at low temperature, comparing with direct methanol fuel cells (DMFCs) [2, 3].

Numerous studies have shown that Pd catalysts accomplish higher activity for formic acid oxidation than Pt [4, 5]. It is generally accepted that that formic acid oxidation occurs on Pd catalysts in line with a direct dehydrogenation reaction mechanism to form CO_2 with less CO-like poisoning species generated, which is different from that on Pt catalysts with the main self-poisoning dehydration reaction pathway [6]. Research in Pd catalysis has mainly focused on addressing Pd deactivation promoted by adsorption of formic acid oxidation by-products. From this research, enhanced activity has been achieved by combination a second metal (such as Au [7], Pt[8], Ir [9]，Pb [10], Sn [11], Co [6], Ni [12], etc) with palladium. The enhancement is mainly due to the weakening of the adsorption of inhibiting reaction intermediates on the catalyst surface, which has been explained by the electronic, strain, or alloying effects [13].

On the other hand, it has been proved that Fe as an assistant component plays an important role in the enhancement of the catalytic activity of noble metals such as Pt and Pd [14-18]. Shao et al. [16] reported that Pd-Fe alloy nanoparticles exhibited an excellent activity for oxygen reduction reaction (ORR). Besides, PtFe alloy nanoparticles exhibit excellent catalytic activities for formic acid electro-oxidation and stability with excellent tolerance to CO poisoning [14]. To the best of our knowledge, however, PdFe bimetallic catalysts for formic acid electro-oxidation have not been reported yet.

The aim of the present work is to synthesize an efficient catalyst of formic acid eletro-oxdation by combining MWCNTs support with promoting palladium by iron. Such a novel catalyst has been synthesized by a simple microwave-assisted polyol method for the first time. The physicochemical properties and electrochemical activities of the catalysts for formic acid electro-oxidation were investigated. The reasons for the enhanced oxidation activity were discussed as well.

2. EXPERIMENTAL PART

2.1. Catalyst preparation

The preparation of xPdyFe/MWCNTs catalysts is briefly described as follows: a calculated amount of 0.01 mol·L^{-1} palladium chloride solution was added dropwise into 50 mL of ethylene glycol, and the pH was adjusted to 11-12 with $NH_3 \cdot H_2O$. Next, a calculated amount of $FeCl_3 \cdot 6H_2O$ was added into the solution and then 80 mg of MWCNTs (BET > 200 m$^2 \cdot$g^{-1}) after the pretreatment described as reference [8], were mixed and ultrasonicated for 1 h. The obtained solution was heated in a microwave for 10 s with 10 s interval breaks for several cycles. Finally, the slurry was filtered and dried under vacuum at 100 °C for 10 h. The setting atomic ratios of Pd to Fe were 3:1, 2:1 and 1:1, respectively. The whole loadings of Pd and Fe in the catalysts were all 20% by weight. For comparison, Pd/MWCNTs (20 wt.% Pd loading) was also prepared using the same method. TEM-EDX showed that the Pd/Fe molar ratios in obtained PdFe/MWCNTs catalysts were 3.4:1, 1.8:1, 0.8:1, respectively.

2.2. Catalyst characterization

Transmission electron microscopy (TEM) was carried out on the JEM-1230 microscope. X-ray diffraction (XRD) was recorded on Philips PW3040/60 X-ray diffractometer with Cu Kα radiation of wavelength λ =0.15406 nm.

All electrochemical measurements were carried out with a CHI 730d electrochemistry workstation at 25 °C. Working electrodes were prepared from 4 mm diameter glassy carbon disc electrodes. The catalyst powders were mixed with deionized water and 5 wt.% Nafion solution, and then coated on a mirror-polished glassy carbon disk electrode. Pt foil and saturated calomel electrode (SCE) were used as counter and reference electrode respectively. The electrolyte used was 1 M H_2SO_4 +1 M HCOOH. For the electrochemical measurement of the absorbed CO, CO was bubbled into the solution for 30 min when the electrode potential was fixed at 0.02 V vs. SCE. Then, N_2 was bubbled into the solution for 30 min to remove the CO in the solution.

3. RESULTS AND DISCUSSION
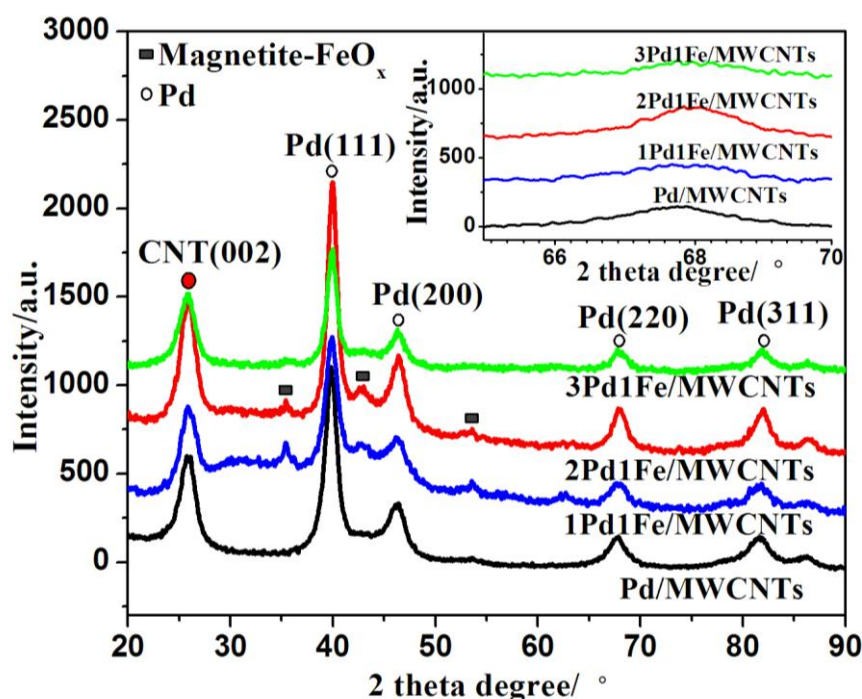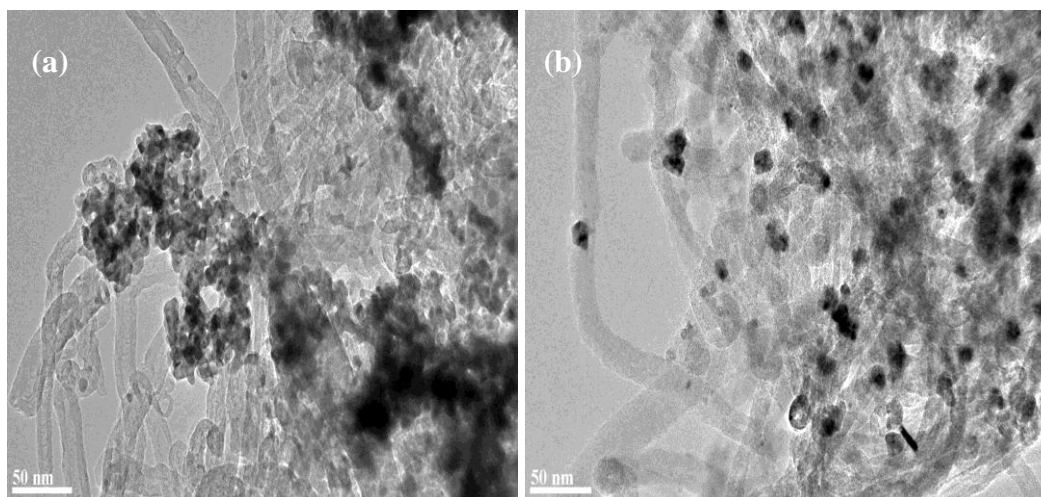
3.1. Physicochemical characterization

Figure 1. XRD patterns of Pd/MWCNTs and PdFe/MWCNTs catalysts with different ratios of Pd/Fe. Inset is an expanded view of the (220) reflections.

Fig. 1 depicts the XRD patterns of Pd/MWCNTs and PdFe/MWCNTs catalysts. As shown, the peak located at a 2θ value of about 26 ° is attributed to the graphite (002) plate of the MWCNTs, and the other four peaks (39.8 °, 46.2 °, 67.8 ° and 81.6 °) are reflections for the face-centered cubic crystal lattice of the (111), (200), (220), (311) facets of palladium crystal. However, the characteristic peaks

for the PdFe/MWCNTs catalysts shift slightly to high 2θ values, compared with those for the Pd/MWCNTs. This indicates that Fe atoms enter into the Pd lattice and PdFe alloy is formed to certain extent. Furthermore, the weak diffraction peaks at 35.2 °, 42.9 ° and 53.3 °, corresponding to (311), (400) and (422) facets of Magnetite non-stoichiometric iron oxides (described as being "FeO_x"), indicate the coexistence of nano-PdFe and nano-FeO_x, and the uncompleted reduction of iron ions in the system. Additionally, the average sizes of Pd particles on 2Pd1Fe/MWCNTs and Pd/MWCNTs are calculated as 8.3 and 6.1 nm respectively from the (111) peak by the Scherrer formula [12].The typical TEM images and the corresponding histograms of Pd/MWCNTs and 2Pd1Fe/MWCNTs are shown in Fig. 2a-2d. As seen, the significant aggregation of Pd particles is observed on Pd/MWCNTs (Fig. 2a), while the agglomeration degree of Pd particles is depressed predominantly and a relatively uniform and high dispersion of metal particles is observed on 2Pd1Fe/MWCNTs (Fig. 2b). The particle size histogram based on measuring over 300 Pd particles shows the Pd/MWCNTs catalyst has a wide particle size dispersion of 2 - 16 nm with the mean particle size of 6.5 nm (Fig. 2c). In contrast, the particle size distribution of 2Pd1Fe/MWCNTs catalyst is narrower, in a range from 4 to 13 nm with mean particle size of 8.2 nm (Fig. 2d).

Fig. 2e provides the representative HRTEM image of 2Pd1Fe/MWCNTs, where the continuous ordered lattice fringes are well resolved. The lattice spacing is calculated to be ~0.222 nm, ~0.200 nm and ~0.250 nm, corresponding to the distance of the (111) facet and (220) facet of Pd nanoparticles, and the (311) facet of nano-FeO_x, respectively. All of the values are in excellent agreement with the standard d values. This means that Fe exists in the catalyst both as FeO_x and PdFe alloy, which is in good agreement with the XRD results. It's worthy mentioning that FeO_x crystallites are in close contact with the alloyed Pd crystallites. Iron oxides form the individual phase and separate the particles of the main phase [17]. Thus, nano-FeO_x can impede the aggregation of Pd particles and facilitate the dispersion of Pd nanoparticles. Palladium, iron and oxygen atoms distribute well on the surface of the catalysts, which can be seen from EDX mapping of selected particles of 2Pd1Fe/MWCNTs presented in Fig. 4f.
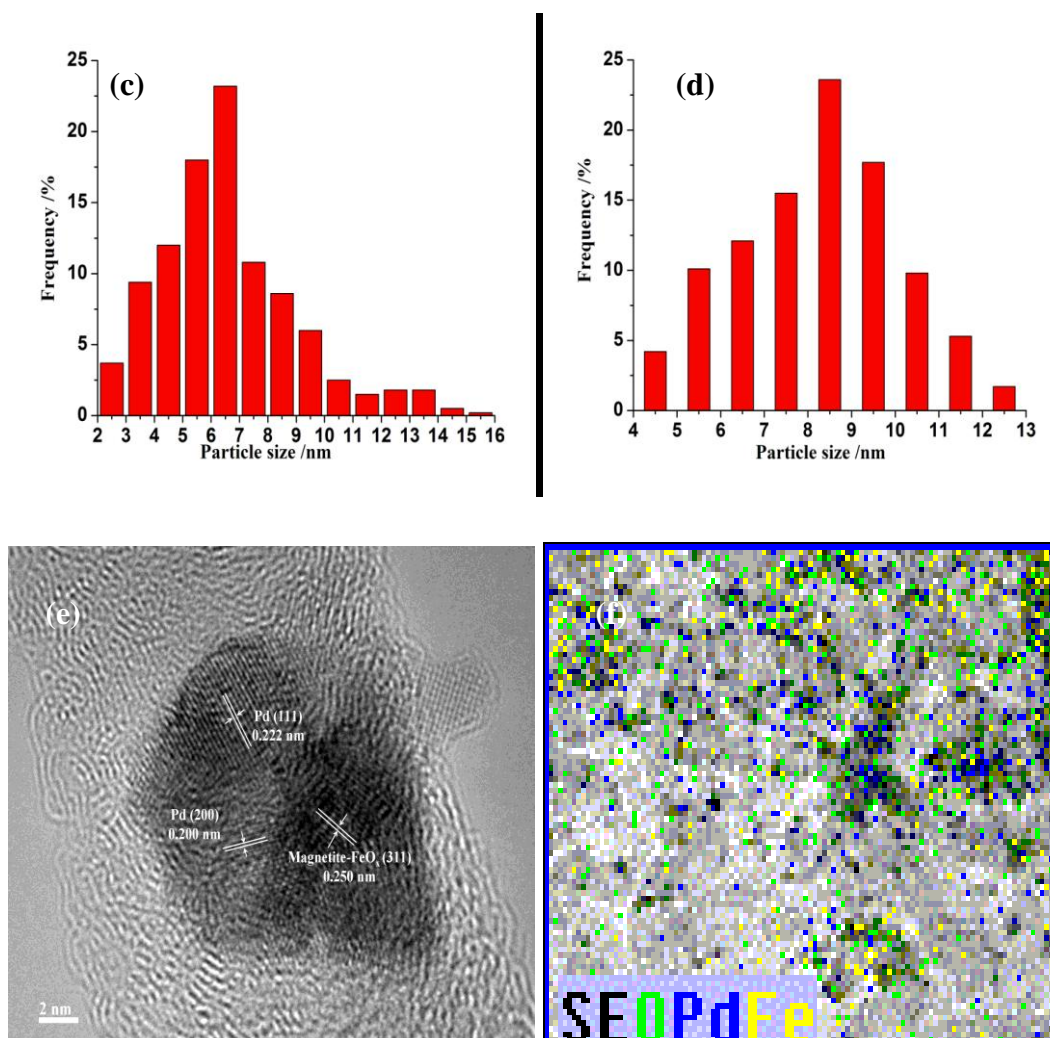
Figure 2. TEM images of (a) Pd/MWCNTs and (b) 2Pd1Fe/MWCNTs; Particle size histograms of (c) Pd/MWCNTs and (d) 2Pd1Fe/MWCNTs; (e) HRTEM image of 2Pd1Fe/MWCNTs; (f) EDX Pd, Fe and O mapping of selected particles of 2Pd1Fe/MWCNTs.

3.2. Electrochemical characterization

The inset in Fig. 3 shows the cyclic voltammograms (CV) in 1 M H_2SO_4 on different electrodes. It is found that the hydrogen adsorption and desorption peaks in the potential interval of 0 – 0.2 V on the 2Pd1Fe/MWCNTs (Pd loading= 0.16 mg·cm^{-2}) electrode is larger than that on Pd/MWCNTs (Pd loading= 0.2 mg·cm^{-2}) electrode, indicating the former has larger electrochemical surface area than the latter. The results further reveal that the adsorption/desorption of hydrogen is more active on 2Pd1Fe/MWCNTs than that on Pd/MWCNTs. In addition, both the electrodes are observed to deliver reduction peaks about 0.4 V, which can be attributed to the reduction of the oxide formed on the Pd during the forward scan [19].

The CV results for the catalysts with different ratios of Pd/Fe in 1 M HCOOH + 1 M H_2SO_4 are shown in Fig. 3. Obviously, no anodic peak is observed at the Fe/MWCNTs catalyst electrode, indicating that Fe/MWCNTs catalyst has no electrocatalytic activity for the oxidation of formic acid.

Large peaks near 0.2 V and small peaks near 0.6 V for all electrodes can be observed on both Pd/MWCNTs and PdFe/MWCNTs catalyst electrodes. The potentials of the main anodic peaks of formic acid at all PdFe/MWCNTs electrodes show 73-125 mV shift to more negative evidently, compared with Pd/MWCNTs electrode. The current densities of the main anodic peak of formic acid are 42.8, 57.0 and 45.5 mA·cm^{-2} at the 1Pd1Fe/MWCNTs, 2Pd1Fe/MWCNTs and 3Pd1Fe/MWCNTs catalyst electrodes, respectively. Among them, 2Pd1Fe/MWCNTs electrode displays the best catalytic activity for formic acid electro-oxidation with the most negative peak potential (0.086 V) and the highest peak current (57 mA·cm^{-2}). The above results illustrated that Fe in the PdFe/MWCNTs catalyst could cause the negative shift of the potential of the main anodic peak of formic acid and the increase in the current density of this peak at the Pd/MWCNTs catalyst.

It was reported that the electrooxidation of formic acid could undergo through two parallel pathways, the direct pathway and the CO pathway [20-21]. The direct pathway is the perfect pathway, because for the direct pathway, formic acid is directly oxidized to CO_2 and no CO intermediate is formed. Thus, the catalyst is not easy to be poisoned. For the Pd/MWCNTs catalyst electrodes, the current density of the peak at 0.19 V is 38.8 mA·cm^{-2} (through the direct pathway), which is much larger than that at about 0.77 V (through the CO pathway), and the ratio is 3.06. While for the 2Pd1Fe/MWCNTs catalyst electrode, the ratio of the current densities of the peaks at 0.086 V and about 0.56 V is 4.92, which is larger than that at the Pd/MWCNTs catalyst electrode (3.06). The results illustrate Fe can promote the oxidation of formic acid on the Pd catalyst through the direct pathway.
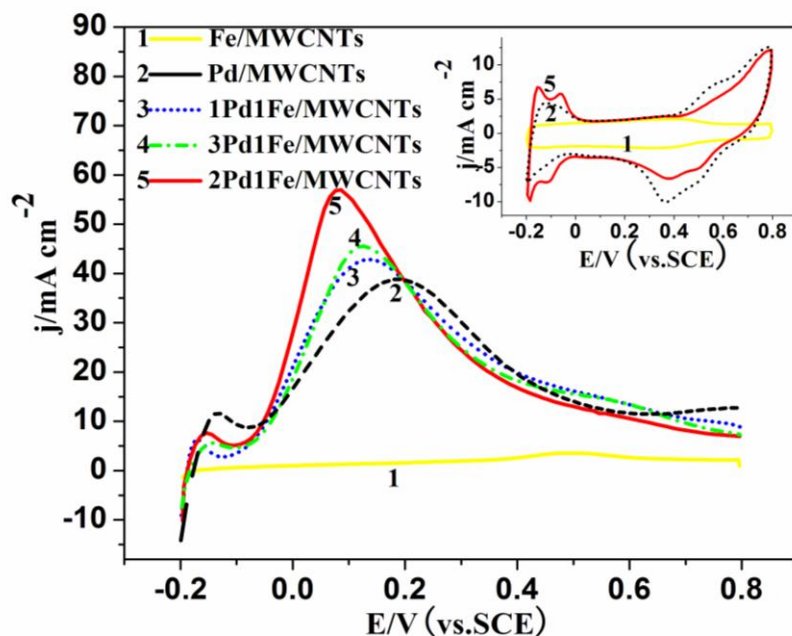

Figure 3. Cyclic voltammograms in 1 M HCOOH + 1 M H_2SO_4 solution for different electrodes. Inset is CV of 1 M H_2SO_4 solution on three electrodes. Scan rate: 50 mV/s.

An electronic (ligand) effect is considered to be able to change the electronic structure and density of state (DOS) of metal catalysts and weaken the bond energy between metal and strongly adsorbed poisons, which has been reported in many literatures [22–25]. The density functional theory calculations indicate that compression of a Pd lattice in PdFe alloys will downshift the d-band center by -0.88 eV [16]. Namely, Fe modifies the electronic structure of Pd and produces an electronic effect by alloy-forming [17], which probably influences the chemisorption energy of intermediates such as .COOH adsorbed on the catalysts, and then results in the enhancing performance by increasing the rate of formic acid oxidation to CO_2 [26, 27].

Catalytic activity is known to be influenced by the size and distribution of the catalytically active noble metal nanoparticles [28]. However, the size effect of Pd nanocatalyst should not be the main cause leading to much higher catalytic activity of the 2Pd1Fe/MWCNTs catalysts for the formic acid electrooxidation than the Pd/ MWCNTs catalyst because Pd particles on Pd/MWCNTs have no great difference from that on 2Pd1Fe/MWCNTs. Otherwise, the relatively narrow and good distribution of Pd particles with almost no aggregation on 2Pd1Fe/MWCNTs catalyst should be another factor of the enhancing performance for the formic acid electrooxidation. The stabilities of formic acid electro-oxidation on PdFe/MWCNTs electrodes were investigated in solution of 1 M H_2SO_4 containing 1 M HCOOH at a constant potential of 0.4 V, as shown in Fig. 4 The rapid current decrease demonstrates the poisoning of the electrocatalysts [19]. The current densities for all PdFe/MWCNTs catalysts are observed to be higher than that for Pd/MWCNTs during 2000 s. And among them, 2Pd1Fe/MWCNTs catalyst is able to maintain the highest current density all the time. This suggests that certain content of Fe enhances the stability and poisoning tolerance of Pd.
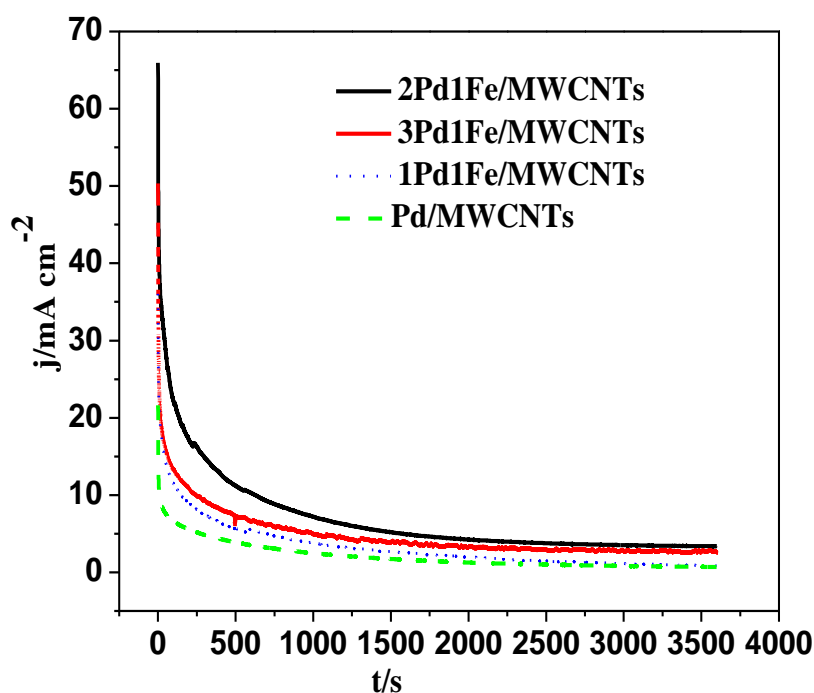

Figure 4. Chronoamperometric curves of PdFe/MWCNTs electrodes in 1 M H_2SO_4 containing 1 M HCOOH at 0.4 V.

In order to evaluate the poisoning effect of CO, CO-stripping cyclic voltammograms of the adsorbed CO at the different catalysts are shown in Fig. 5. No anodic peak is observed at the Fe/MWCNTs catalyst, indicating that CO cannot be adsorbed on the Fe surface. At the Pd/MWCNTs catalyst electrode, a strong anodic peak of adsorbed CO is located at 0.84 V, illustrating that CO can be strongly adsorbed on the Pd surface [29]. At the 2Pd1Fe/MWCNTs catalyst electrode, the anodic peak of the adsorbed CO is located at 0.75 V, which is 90 mV more negative than that at the Pd/MWCNTs catalyst electrode. This is an indication that that even small amount of Fe exists in the Pd lattice, the adsorption strength of CO on Pd would be significantly decreased. The weakened strength of CO adsorption on the catalyst prevents the accumulation of poisoning intermediates. Thus, more active sites are available for the formic acid electro-oxidation via the direct pathway, which results in a remarkable enhancement of the activity.
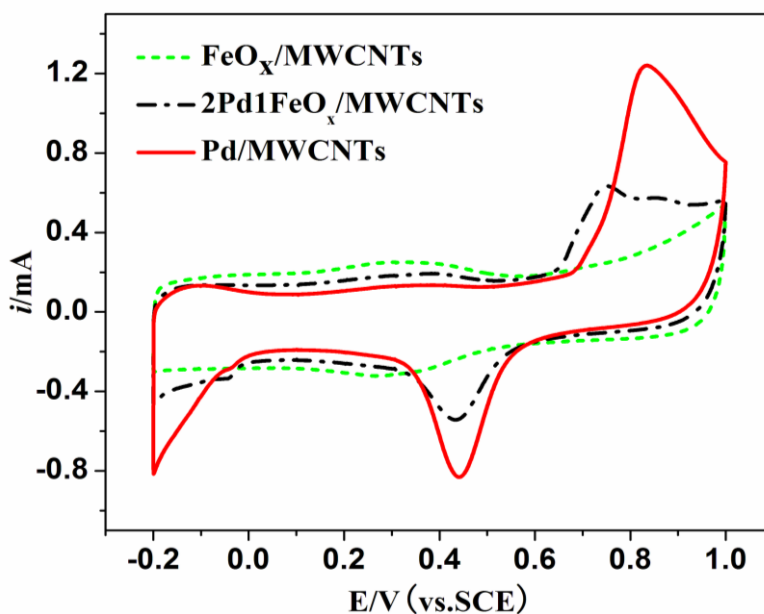

Figure 5. CO stripping cyclic voltammograms on different electrodes in 0.5 M H_2SO_4 with scan rate of 50 mV/s.

4. CONCLUSIONS

The novel MWCNTs supported PdFe catalysts were prepared by a simple microwave-assisted polyol method for the first time. The electrocatalysts were characterized by X-ray diffraction (XRD) and transmission electron microscopy (TEM). According to the XRD and TEM results, Pd particles on Pd/MWCNTs have a wide particle size distribution of 2-16 nm with significant aggregation, while 2Pd1Fe/MWCNTs catalyst has a relatively narrow distribution of particles in a range of 4-13 nm, centers at 8.2 nm, and the particles are composed mainly of PdFe and FeO_x crystallites with uniformity and high dispersion. The results of electrochemical analysis illustrate that the addition of Fe can

improve both the activity and the stability of PdFe/MWCNTs catalysts. So, occurrence of iron can influence on the activity of catalyst by two ways: (1) The electronic effect of Fe decreases the adsorption strength of both the formate intermediate and CO on Pd, which can enhance the rate of the HCOOH molecule decomposition via the direct path. (2) Nano-FeO_x can impede the aggregation of Pd particles and facilitate the dispersion of Pd nanoparticles, which helps to improve the performance for the formic acid electrooxidation.

References

1. C. Rice, S. Ha and R. I. Masel, A. Wieckowski, *J. Power Sources*, 115 (2003) 229.
2. X. Yu and P. G. Pickup, *J. Power Sources*, 182 (2008) 124.
3. S. Ha, B. Adams and R. I. Masel, *J. Power Sources*, 128 (2004) 119.
4. Z. Liu, L. Hong, M.P. Tham, T.H. Lim and H. Jiang, *J. Power Sources*, 161 (2006) 835.
5. P. K. Babu, H. S. Kim, J. H. Chung, E. Oldfield and A. Wieckowski, *J. Phys. Chem. B*, 108 (2004) 20228.
6. D. Morales-Acosta, M.D. Morales-Acosta, L.A. Godinez, L. álvarez-Contreras, S.M. Duron-Torres, J. Ledesma-García and L.G. Arriaga, J. *Power Sources*, 196 (2011) 9270.
7. Q. G. He, W. Chen, S. Mukerjee, S. W. Chen and F. Laufek, *J. Power Sources*, 187 (2009) 298.
8. [8] O. Winjobi, Z. Y. Zhang, C. H. Liang and W. Z. Li, *Electrochim. Acta*, 55 (2010) 4217.
9. X .Wang, Y. Tang, Y. Gao and T. H. Lu, *J. Power Sources*, 175 (2008) 78.
10. X.W. Yu and P.G. Pickup, *J. Power Sources*, 192 (2009) 279.
11. Z. L. Liu, X. H. Zhang, *Electrochem. Commun.*, 11 (2009) 1667.
12. C. Y. Du, M. Chen, W. G. Wang, G. P. Yin, P. F. Shi, *Electrochem. Commun.*, 12 (2010) 843.
13. C. X. Xu, Y. Q. Liu, J. P. Wang and H. R. Geng, H. J. Qiu, *J. Power Sources*, 199 (2012) 124.
14. W. Chen, J. Kim, S. H. Sun and S. W. Chen, *Langmuir*, 23 (2007) 11303.
15. X. Wang and R.J. Gorte, *App.Catal. A: General*, 247 (2003) 157.
16. M. H. Shao, K. Sasaki and R. R. Adzic, *J. Am. Chem. Soc.*, 128 (2006) 3526.
17. M. R. Tarasevich, G. V. Zhutaeva, V. A. Bogdanovskaya, M. V. Radina, M. R. Ehrenburg and A. E. Chalykh, *Electrochim. Acta*, 52 (2007) 5108.
18. W. Z. Li, W. J. Zhou, H. Q. Li, Z.H. Zhou, B. Zhou, G. Q. Sun, Q. Xin，*Electrochim. Acta*, 49 (2004) 1045.
19. S. X. Zhang, M. Qing , H. Zhang and Y. N. Tian, *Electrochem. Commun.*, 11 (2009) 2249.
20. S. Ha, R. Larsen, Y. Zhu and R.I. Masel, *Fuel Cells*, 4 (2004) 337.
21. S. Ha, R. Larsen and R.I. Masel, *J. Power Sources*, 144 (2005) 28.
22. T. Frelink, W. Visscher and J. A. R. van Veen, *Surf. Sci.*, 335 (1995) 353.
23. E. Herrero, M. J. Llorca, J. M. Feliu and A. Aldaz, *J. Electroanal.Chem.*, 394 (1995) 161.
24. K. W. Park, J. H. Choi, B. K. Kwon, S. A. Lee, Y. E. Sung, H. Y. Ha, S. A. Hong, H. Kim and A. Wieckowski, *J. Phys.Chem. B*, 106 (2002)1869.
25. V. Stamenkovic, B. S. Mun, K. J. J. Mayrhofer, P. N.Ross, N. M. Markovic, J.Rossmeisl, J. Greeley and J. K.Norskov, *Angew. Chem., Int. Ed.*, 45 (2006) 2897.

26. Z. H. Zhang, J. J. Ge, L. A. Ma, J. H. Liao, T. H. Lu and W. Xing, *Fuel Cells*, 9 (2009) 114.
27. W. P. Zhou, A. Lewera, R. Larsen, R. I. Masel, P. S. Bagus and A. Wieckowski, *J. Phys. Chem. B*, 110 (2006) 13393.
28. T. S. Ahmadi, Z. L. Wang, T. C. Green, A. Henglein, M. A. El-Sayed. *Science*, 272 (1996) 1924.
29. X. Wang, Y. Tang, Y. Gao, T. Lu, *J. Power Sources*, 175 (2008) 784.